Iridium Coating Deposited by Double Glow Plasma Technique — Effect of Glow Plasma on Structure of Coating at Single Substrate Edge

2012 Plasma Sci. Technol. 14 909

(http://iopscience.iop.org/1009-0630/14/10/10)

Iridium Coating Deposited by Double Glow Plasma Technique*

— Effect of Glow Plasma on Structure of Coating at Single Substrate Edge

WU Wangping (吴王平), CHEN Zhaofeng (陈照峰), LIU Yong (刘勇)

College of Material Science and Technology, Nanjing University of Aeronautics and Astronautics, Nanjing 210016, China

Abstract Double glow plasma technique has a high deposition rate for preparing iridium coating. However, the glow plasma can influence the structure of the coating at the single substrate edge. In this study, the iridium coating was prepared by double glow plasma on the surface of single niobium substrate. The microstructure of iridium coating at the substrate edge was observed by scanning electron microscopy. The composition of the coating was confirmed by energy dispersive spectroscopy and X-ray diffraction. There was a boundary between the coating and the substrate edge. The covered area for the iridium coating at the substrate edge became fewer and fewer from the inner area to the outer flange-area. The bamboo sprout-like particles on the surface of the substrate edge were composed of elemental niobium. The substrate edge was composed of the Nb coating and there was a transition zone between the Ir coating and the Nb coating. The interesting phenomenon of the substrate edge could be attributed to the effects of the bias voltages and the plasma cloud in the deposition chamber. The substrate edge effect could be mitigated or eliminated by adding lots of small niobium plates around the substrate in a deposition process.

Keywords: glow plasma, coating, iridium, niobium

PACS: *52.20.Hv, 52.50.Nr, 52.80.Vp*

DOI: 10.1088/1009-0630/14/10/10

1 Introduction

Iridium (Ir) is noted as having a high melting temperature, high elastic modulus, superior hardness, high tensile strength at room temperature, excellent chemical stability, low oxygen permeability and very low electrical resistivity [1,2]. Ir acts as an effective diffusion barrier for inward-moving oxygen and outward-moving carbon for some materials [3,4]. Many of features of Ir make it suitable for protecting structural materials from high temperature damage in order to prolong service life [5,6]. Ir is one of the most promising candidates for protective coating of either structural carbon material or rhenium (Re) rocket thrusters against extreme environments. At present, one successful application of Ir coating is its use in a liquid rocket motor. Ultramet's flagship product Ir/Re combustion chamber can operate at temperatures up to 2200°C [7]. Many methods can be used to prepare Ir coating, such as metal organic chemical vapor deposition (MOCVD) [8,9], CVD [10], electron beam evaporation [11,12], sputtering [13,14], pulsed laser deposition [15,16], laser-induced chemical decomposition [17], electroformed deposition [18] or the double glow plasma technique [19~21].

In previous work, Ir coating was used for high-temperature oxidation resistance coatings, which were deposited by a double glow plasma technique on the surface of refractory metals and carbonaceous materials [22~25]. Microstructure, mechanical and oxidation properties of the Ir coating have been deeply investigated. However, many experimental results from the preparation of Ir coating show that the glow plasma has a significant impact on the structure of the coating at the single substrate edge, which has so far been unpublished in literatures. In the present work the Ir coating was deposited by using the double glow plasma technique on the surface of a niobium (Nb) substrate. The effect of glow plasma on the structure of the coating at the single substrate edge was investigated.

2 Experimental procedure

Double glow plasma technique, also called as Xu-Tec, can be regarded as a new kind of physical vapor deposition, which could apply almost all solid metallic elements to realize surface alloying of the metallic substrates [18]. The general advantages of this technique include low cost, high deposition rate, surface smoothness, good coating uniformity, controllability of the coating thickness and strong adhesion to the substrate. A detailed description of double glow plasma device was reported elsewhere [19,20]. The surface alloying experiment was performed in a double glow plasma surface alloying device, in which low temperature plasma was produced by a glow discharge process in a vacuum sputtering chamber. Three electrodes were de-

*supported by National Natural Science Foundation of China (50872055/E020703), Funding for Outstanding Doctoral Dissertation in NUAA (BCXJ11-09), the Fundamental Research Funds for the Central Universities and Funding of Jiangsu Innovation Program for Graduate Education of China (CXLX11_0207)

signed in the chamber: one anode and two negatively charged members, the work-piece is one cathode (substrate) and the desired coating material is another one (target). Both the target and the substrate are the cathode electrodes. When two different voltages are applied to the two cathode electrodes, the target and substrate are surrounded respectively by their own glow discharge. The target material was sputtered by the high energy Ar^+ for supplying the sputtering atoms. The sputtered atoms move toward the substrate and an excellent coating is formed on the surface of the substrate. An Ir plate (purity: 99.95%, $\phi 50 \times 3.5$ mm) was used as the target material. Nb plates ($16 \times 16 \times 4$ mm) were used as the substrate materials. In this experiment, only one substrate was laid on the surface of the base plate in a deposition process. Before deposition, the substrates were all re-polished by metallographic abrasive paper ($5 \sim 20$ μm) and then by using 1μm diamond media. The polished substrates were cleaned ultrasonically in acetone and then dried in an oven for 1 h at 80 °C in order to remove acetone from the substrate. Argon was used as the working gas. The deposition conditions were: base pressure 4×10^{-4} Pa, target bias voltage $-800 \sim -850$ V, substrate bias voltage $-300 \sim -350$ V, working gas pressure 35 Pa, parallel distance between Ir target and the substrate 15 mm, deposition time 2 h.

The microstructure of the coating at the substrate edge was observed by scanning electron microscopy (SEM, FEI CO., Quanta200, JSM-6360LV). The phase identification of the coating was determined by X-ray diffraction (XRD, Rigaku D/Max-B) using Ni-filtered Cu K_α radiation. The chemical composition of the coating was examined by energy dispersive spectroscopy (EDS, LINK-860).

3 Results

Fig. 1 shows the XRD pattern and SEM micrograph of Nb substrate. According to standard JCPDS Card (No. 35-0789), the substrate was composed of polycrystalline Nb (Fig. 1(a)). Nb(110), Nb(200), Nb(211) and Nb(220) diffraction peaks appeared in the XRD pattern. The surface of the polished substrate appeared smooth by visual observation, but some scratched lines could be observed as shown in Fig. 1(b).

Fig. 2 presents the XRD pattern and SEM micrographs of the Ir coating at the center of the as-coated specimen. Compared with the standard d-values taken from JCPDS Card (No. 46-1044), the as-deposited Ir coating has a polycrystalline structure (Fig. 2(a)). This indicates the Ir coating had a dominating (220) orientation. The other diffraction peaks were very weak. The surface of the coating was composed of many small aggregates. No microcracks and pores were observed on the surface of the coating (Fig. 2(b)). The fracture surface of the coating shows an array of columnar grains aligned perpendicular to the substrate surface. The

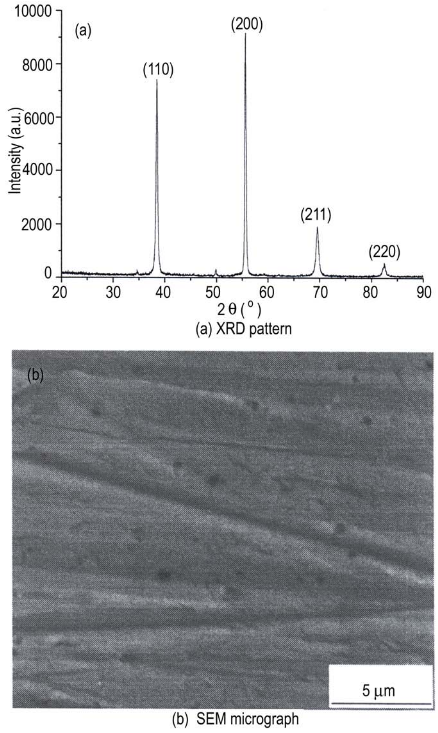

Fig.1 (a) pattern and (b) SEM micrograph of the Nb substrate

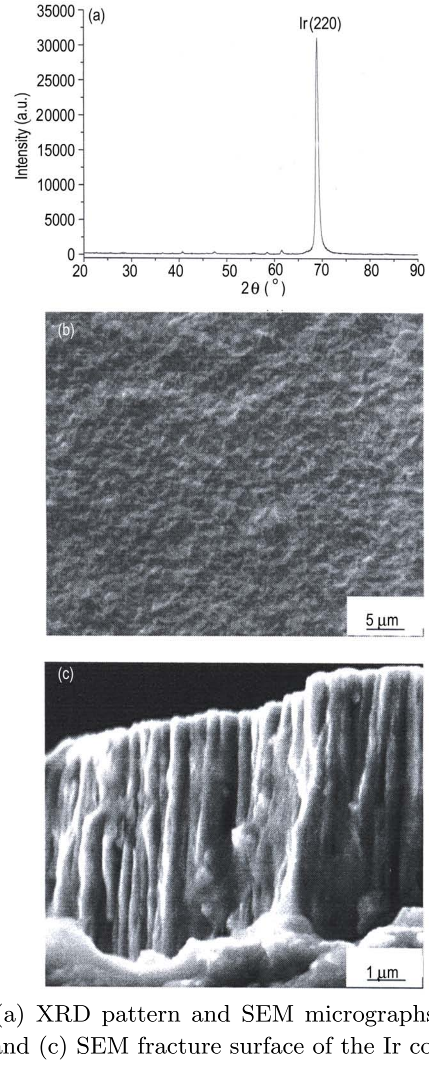

Fig.2 (a) XRD pattern and SEM micrographs (b) SEM surface and (c) SEM fracture surface of the Ir coating

columnar grains extended through the entire coating thickness. Some columnar grains were broken by external stress. It could be observed that the thickness of the coating was approximately 8 μm.

Fig. 3 shows the micrographs of the coating at the substrate edge. There was a boundary between the Ir coating and the Nb coating. It was found that many particles were presented on the surface of the Nb coating. The morphologies of the Ir coating and the Nb coating were dramatically different. As shown in Fig. 3, these particles presented regular growth direction. The Nb coating was composed of large bamboo sprout-like

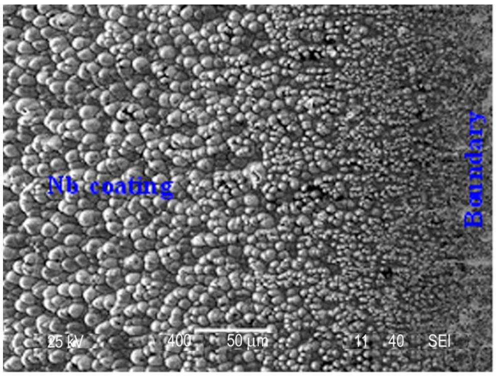

Fig.3 Micrograph of the surface of the substrate at the substrate edge

particles with sizes in the range of 10∼20 μm and small particles with sizes in the range of 0.5∼1 μm. The particle sizes near the boundary were smaller than that outside of the Nb coating, which could be the effects of the resputtering and glow plasma cloud in the deposition chamber. Resputtering could result in redeposition of the substrate element on the surface of the substrate.

Fig. 4 shows the backscatter electron photographs and EDS spectra of the Nb coating at the substrate edge. The surface of the Nb coating was composed of 6∼10 μm grains together with many smaller grains interspersed among the larger grains. Some white aggregates appeared on the surface of big bamboo sprout-like particles. The EDS spectrum indicated that the bamboo sprout-like particles were mainly composed of elemental Nb and few elemental Ti (Fig. 4(c)). From Fig. 4(b), it can be found that the white aggregates were not well-proportioned. Although the white aggregates were massed in the mountainside, they were not formed on the surface of the many smaller grains interspersed among the larger grains. The EDS spectrum indicated that the white aggregates were composed of element Ir (Fig. 4(d)). Fig. 5 shows the SEM micrograph of the cross section of the Ir coating at the middle of the as-coated specimen. It can be found that there was a Nb coating between the Ir coating and the Nb substrate. Furthermore, there was a transition zone between the Ir coating and the Nb substrate. WANG et al. [20] studied the growth mechanism of the transition zone between the Ir coating and the Nb substrate.

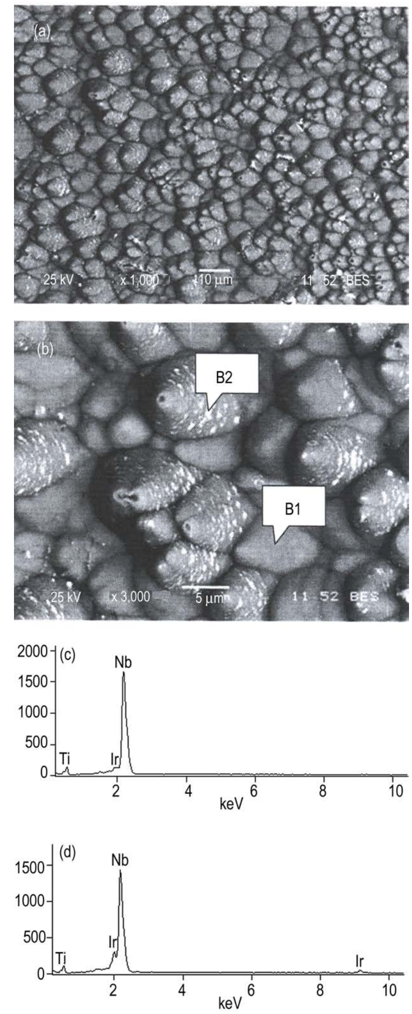

(a) Low magnetication, (b) Large magnetication, (c) B1 dot, (d) B2 dot

Fig.4 Backscatter electron photographs and EDS spectra of the Nb coating at the substrate edge

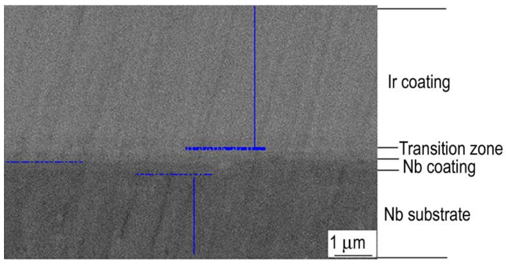

Fig.5 SEM micrographs of cross section of Ir coating at the middle of the as-coated specimen

Fig. 6 shows the micrographs of the boundary between the Ir coating and the Nb coating. It could be found that the grey zone was surrounded by the white zone (Fig. 6(a)). The grey and white areas were composed of the Nb coating and the Ir coating, respectively. It was found that the Ir coating was uncovered on the top of the Nb particles. It can be inferred that the Ir and Nb coatings became a mixed layer until a pure Ir coating was formed on the surface of the substrate. The covered area of the Ir coating became fewer and fewer from the inner area to the outer area. This interesting phenomenon could also be found for depositing Ir coating at other substrate edges, e.g. the sintered tungsten carbide (WC). Fig. 7 shows the SEM micrographs of the WC substrate edge after deposition. The WC coating seemed to be formed at the substrate edge. Many large particles were composed of bamboo sprout-like aggregates. The morphology of these particles was similar to that of the surface of the Nb substrate edge. However, some particles were broken to form many pores on the surface of the substrate edge.

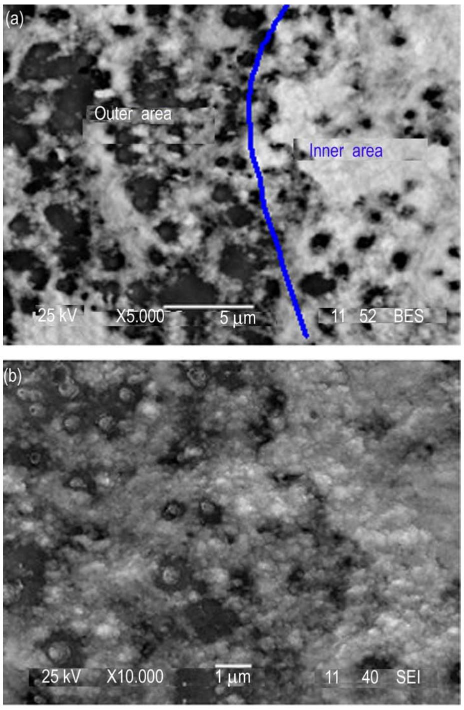

(a) Backscatter electron photograph; (b) SEM micrograph
Fig.6 Micrographs of the boundary between the Ir coating and the Nb coating

4 Discussion

Fig. 8 shows the photographs of the double glow discharge phenomenon during the deposition process. The upper plate was the Ir target and the lower plate was the Nb substrate. The total system was in a high vacuum condition. Firstly, the substrate bias voltage was turned on and one glow was discharged to heat and clean the substrate, which was beneficial to the deposition of Ir element (Fig. 8(b)). It could be found that the substrate and base plate were surrounded by the glow plasma, and the glow plasma at the flange of the substrate and the base plate had edges and corners. Then, when −300 V voltage was applied to the Ir target and the Nb substrate, the rarefied argon was ionized by the accelerated electrons from the cathode electrodes to form the glow plasmas. Both the Ir target and the Nb substrate were surrounded by their own glow plasma to form the double glow plasma (Fig. 8(c)). Here, the glow plasma for the substrate had no edges and cores. The substrate was surrounded by arc-shape glow plasma.

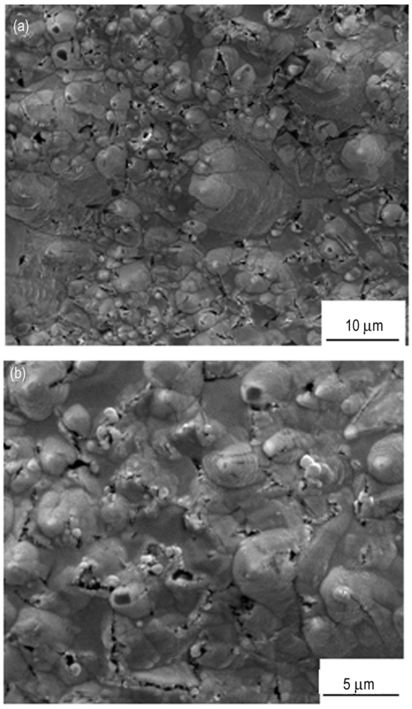

(a) Low magnification, (b) Large magnification
Fig.7 SEM micrographs of the WC substrate edge after deposition

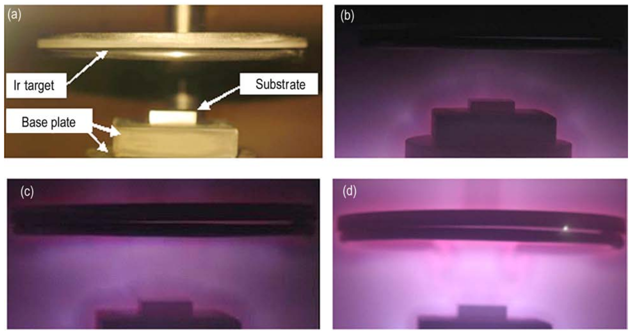

(a) Before deposition, (b) Single glow plasma, (c) Double glow plasma, (d) Cross-linked hybrid plasma
Fig.8 Photographs of the double glow discharge phenomenon during deposition process (color online)

Both the target surface and the substrate surface were synchronously sputtered by the Ar^{+} to produce neutral particles or individual atoms and form glow discharge. Lastly, when the bias voltage of the Ir target was increased to −850 V, the enhanced Ir glow was cross-linked with the Nb glow to form a hybrid plasma region (Fig. 8(d)). The double glow plasma looked like a burning flame from the surface of the substrate. The enhanced discharge could be excited by the cross-linked glow and then increased the plasma density. Because the bias voltage of the Ir target was higher than that of the Nb substrate and the sputtering rate of the Ir element was higher than that of the Nb element, Nb glow discharge was suppressed by intense Ir glow discharge. The Nb atoms in Nb glow discharge were deposited to form Nb coating (Fig. 5). With the Nb and

Ir co-depostion, the Nb element in the as-deposited film gradually decreased and resulted in the formation of a transition zone between the Ir coating and the Nb coating. The Ir atoms in the hybrid plasma cloud were then deposited to form Ir coating.

The Ir glow cross-linked with Nb glow could form a hybrid plasma cloud. The substrate edge seemed not to be surrounded by the strong plasma cloud. The sputtered Nb atoms in the glow cloud were also deposited on the Nb substrate to form the Nb coating, but the number of Nb atoms was less than that of the Ir atoms. The morphological difference of the Nb coating and Ir coating resulted from the effects of the bias voltages and plasma cloud. The central zone of the Nb substrate was covered by the hybrid Ir plasma cloud and subsequently obtained a transition zone and finally produced a pure Ir coating. In general, the flange discharge effect was bigger than that of plane surface of the substrate. Because the plasma cloud did not completely cover and surround the substrate, especially, the flange or the edgewise corner where the glow cloud was relatively strong, the substrate edge was deposited by the sputtered Nb atoms to obtain Nb coating. The substrate edge effect could be overcome by adding other Nb plates near the substrate to make the flange outshift.

Fig. 9 shows a schematic diagram of the plasma cloud. The Nb atoms were also excited and deposited on the Nb substrate to form a Nb coating. According to the above discussion about Fig. 8, the substrate bias voltage was first applied, and then the whole surface of the Nb substrate was sputtered out. However, the target bias voltage began to be applied, and then the Nb and Ir were co-sputtered out. This resulted in the formation of a transition zone between the Ir coating and the Nb coating (Fig. 5). Because of the large difference between the target bias voltage and the substrate bias voltage, sputtered Nb and Ir atoms formed on the surface of the substrate with time and temperature. However, the target bias voltage was higher than the substrate bias voltage, which resulted in higher sputtering rate for the Ir target. Nb atoms were suppressed by the denser Ir atoms and formed a mixed boundary layer on the Nb substrate surface. Therefore, the central zone was covered by the Ir plasma cloud and pure Ir coating was obtained. The marginal zone was not covered by the Ir plasma cloud and contained the as-deposited Nb coating, which was attributed to the effect of the bias voltages. In the experiment, the dividing line of the plasma cloud was not clear, but the substrate had a clear area which was not covered by Ir coating.

5 Conclusion

Ir coating was prepared by double glow plasma on the surface of a Nb substrate. The influence of the glow plasma on the structure of the substrate edge was investigated. There was a boundary between the Ir

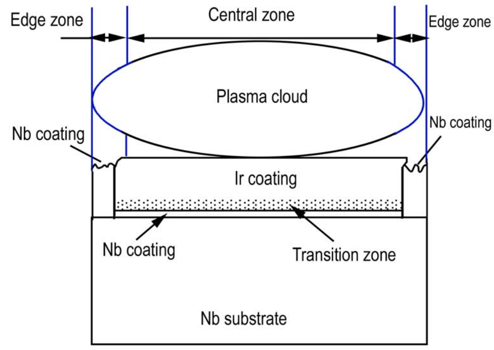

Fig.9 Schematic diagram of the plasma cloud

coating and the substrate edge. The area of the covered Ir coating at the substrate edge became fewer and fewer from the inner area to the outer area. The flower buds-like particles of the substrate edge were composed of element niobium. The particles presented a regular growth direction. The substrate edge was composed of the Nb coating and there was a transition zone between the Ir coating and the Nb coating. For the deposition of Ir coating, this phenomenon was also found on other substrate edges. This phenomenon for the free-Ir coating portion could be attributed to the effects of the bias voltages and the plasma cloud in the deposition chamber. The substrate edge effect could be mitigated or eliminated by adding lots of small substrates over the base plate in a deposition process.

References

1 Mumtaz K, Echigoya J, Taya M. 1993, J. Mater. Sci., 28: 5521
2 Kuppusami P, Murakami H, Ohmura T. 2004, J. Vac. Sci. Technol. A, 22: 1028
3 Hua Y F, Zhang L T, Cheng L F, et al. 2005, Mater. Sci. Eng. B, 121: 156
4 Wu W P, Lin X, Chen Z F, et al. 2011, Plasma Chem. Plasma Process., 31: 465
5 Chen Z F, Wu W P, Cheng H, et al. 2010, Acta Astron., 66: 682
6 Wu W P, Chen Z F, Cheng H, et al. 2011, Appl. Surf. Sci., 257: 7295
7 http://www.ultramet.com/propulsionsystem_components_liquid_rocket.html
8 Vargas R, Goto T, Zhang W, et al. 1994, Appl. Phys. Lett., 65: 1094
9 Gelfond N V, Tuzikov F V, Igumenov I K. 1993, Thin Solid Films, 227: 144
10 Hamilton J C, Yang N Y C, Clift W M, et al. 1992, Metall. Mater. Trans. A, 23: 851
11 Gregory T, Christopher W, Storment J. 1992, IEEE Trans. Biomed. Eng., 39: 893
12 Reeves G K, Lawn M W, Elliman R G. 1992, J. Vac. Sci. Technol. A, 10: 3203
13 El Khakani M A, Chaker M, Le Drogoff B. 1998, J. Vac. Sci. Technol. A, 16: 885
14 Mumtaz K, Echigoya J. 1993, Mater. Sci. Eng. A, 167: 187

15 Galeazzi M, Chen C, Cohn J L, et al. 2004, Nucl. Instrum. Methods Phys. Res. A, 520: 293
16 Gong Y S, Wang C B, Shen Q, et al. 2008, Vacuum, 82: 594
17 Lloyd S, Avery N, Pal M. 2001, Carbon, 39: 991
18 Brian D, Reed R D. 1996, NASA Technical Memorandum, N107172, p. 12
19 Zhang Y, Chen Z F, Wang L B, et al. 2009, J. Coat. Technol. Res., 6: 237
20 Wang L B, Chen Z F, Zhang Y, et al. 2009, Int. J. Refract. Met., 27: 590
21 Zhang Y, Chen Z F, Wang L B, et al. 2009, Fusion Eng. Design., 84: 15
22 Chen Z F, Wu W P, Cong X N, et al. 2011, Advanced Materials Research, 314-316: 214
23 Wu W P, Chen Z F, Lin X. 2011, Advanced Materials Research, 189-193: 688
24 Chen Z F, Wu W P, Wang L B, et al. 2008, Inter. J. Fract., 153: 185
25 Wang L B, Chen Z F, Zhang P Z, et al. 2009, J. Coat. Technol. Res., 6: 517

(Manuscript received 23 September 2011)
(Manuscript accepted 7 November 2011)
E-mail address of corresponding author
CHEN Zhaofeng: zhaofeng_chen@163.com